catalysts

MDPI

Supporting Information

Atomically Dispersed Pd Sites on ZrO_2 Hybridized N-Doped Carbon for Efficient Suzuki–Miyaura Reaction

Jiaqi Du [1], Yidan Peng [1], Xu Guo [1], Guoliang Zhang [1,2,3], Fengbao Zhang [1,2,3], Xiaobin Fan [1,2,3], Wenchao Peng [1,2,3] and Yang Li [1,2,3,*]

[1] School of Chemical Engineering and Technology, Tianjin University, Tianjin 300354, China
[2] Haihe Laboratory of Sustainable Chemical Transformations, Tianjin 300192, China
[3] Institute of Shaoxing, Tianjin University, Zhejiang 312300, China
* Correspondence: liyang1895@tju.edu.cn

Experimental Section

Characterization

X-ray diffraction (XRD) spectra were recorded on a D8-Focus using Cu Kα radiation with a scanning angel (2θ) of 5°–90°. The morphologies of the synthesized catalyst were characterized by scanning electron microscopy (SEM) and transmission electronic microscopy (TEM). SEM images were obtained on a Hitachi S-4800 instrument with an accelerating voltage of 3 kV. TEM, high-resolution TEM (HRTEM) images and the elemental mapping were performed on a JEM-2100F transmission electron microscope at an accelerating voltage of 200 kV. The aberration corrected high-angle annular dark-field scanning transmission electron microscope (HAADF-STEM) images were acquired on a JEM-ARM200F microscope equipped with a spherical aberration corrector at 200 kV. Nitrogen sorption isotherms were obtained on a BJBulider SSA−7000. Surface functional groups were studied with Fourier transform infrared (FTIR) spectroscopy on a Thermo Scientific Nicolet iS20 FTIR spectrometer. Electron Paramagnetic Resonance (EPR) spectra were performed on Bruker EMXplus-6/1 EPR spectrometer. X-ray photoelectron spectroscopy (XPS) results were recorded by an ESCALAB 250Xi photoelectron spectrometer (ThermoFischer) with Al Kα (1486.6 eV) radiation, and all the binding energies obtained in the XPS spectral were calibrated with the standard of the C 1s peak (284.8 eV). The inductively coupled plasma mass spectrometry (ICP-MS) measurement was conducted to determine the Pd contents in the synthesized sample. Raman spectra were collected on a Horiba LabRAM HR Evolution instrument. Details of characterizing the solid phase with X-ray absorption fine structure (XAFS) analyses. Pd K-edge analysis was performed with Si (311) crystal monochromators at the BL14W1 beamlines at the Shanghai Synchrotron Radiation Facility (SSRF) (Shanghai, China). Before the analysis at the beamline, samples were pressed into thin sheets with 1 cm in diameter and sealed using Kapton tape film. The XAFS spectra were recorded at room temperature using a 4-channel Silicon Drift Detector (SDD) Bruker 5040. Pd K-edge extended X-ray absorption fine structure (EXAFS) spectra were recorded in fluorescence mode. Negligible changes in the line-shape and peak position of Pd K-edge XANES spectra were observed between two scans taken for a specific sample. The XAFS spectra of these standard samples (Pd foil and PdO) were recorded in transmission mode. The spectra were processed and analyzed by the software codes Athena and Artemis. The obtained XAFS data was processed in Athena (version 0.9.26) for background, pre-edge line and post-edge line calibrations. Then Fourier transformed fitting was carried out in Artemis (version 0.9.26). The k^3 weighting, k-range of 3.0 - 12.3 $A^{\circ-1}$ and R range of 1.1 – 2.5 Å were used for the fitting. The four parameters, coordination number, bond length, Debye-Waller factor and E0 shift (CN, R, σ^2, ΔE_0) were fitted without anyone was fixed, constrained, or correlated. For Wavelet Transform analysis, the $\chi(k)$ exported from Athena was imported into the Hama Fortran code. The parameters

were listed as follow: R range, 1 - 3.5 Å, k range, 0 - 13 $Å^{-1}$ for Pd foil and PdO; k weight, 2; and Morlet function with κ=10, σ=1 was used as the mother wavelet to provide the overall distribution. The reactions were monitored by an Agilent 6890N GC equipped with HP-5 capillary.

Synthetic procedures

Synthesis of Pd/N–C

The synthesized sample of Pd@ZrO_2/N–C was dispersed in 120 mL of H_2O containing 0.8 mol HF and stirred for 2 h, followed by centrifugation at 11000 rpm for 5 min. Subsequently, the resultant product was washed with methanol and H_2O (v/v= 1:4) for three times and then dried under vacuum at 80 ℃. The black powder was collected for further use.

Synthesis of UiO-66–NH_2

$ZrCl_4$ (85.6 mg, 0.36 mmol) and H_2BDC-NH_2 (66.5 mg, 0.36 mmol) were dissolved in 80 mL DMF containing 9.6 mL HAc in a 100 mL glass vial. The mixed solution was sonicated for 30 minutes and packed in a 100 mL Teflon-lined autoclave. The autoclave was then sealed and heated in an oven at 120°C for 24 h. Then the product was centrifugated at 11000 rpm for 5 min and washed with a mixture of methanol and DMF (v/v =1:4) for 3 times, finally dried under vacuum at 90 ℃.

Synthesis of ZrO_2/N–C

UiO-66–NH_2 powder was placed in a tube furnace and heated to 700°C at a rate of 5°C/min under a flowing nitrogen atmosphere, then treated at 700°C for another 3 h. After cooling to room temperature, the black powder was collected for subsequent characterization and catalytic testing.

Synthesis of $PdCl_2$/UiO-66

$PdCl_2$ (250μl, 1mg/ml DMF), $ZrCl_4$ (85.6 mg, 0.36 mmol) and H_2BDC (60.4 mg, 0.36 mmol) were dissolved in 80 mL DMF containing 9.6 mL HAc in a 100 mL glass vial. The mixed solution was sonicated for 30 minutes and packed in a 100 mL Teflon-lined autoclave. The autoclave was then sealed and heated in an oven at 120°C for 24 h. Then the product was centrifugated at 11000 rpm for 5 min and washed with a mixture of methanol and DMF (v/v =1:4) for 3 times, finally dried under vacuum at 90 ℃.

Synthesis of Pd@ZrO_2/C

$PdCl_2$/UiO-66 powder was placed in a tube furnace and heated to 700°C at a rate of 5°C/min under a flowing nitrogen atmosphere, then treated at 700°C for another 3 h. After cooling to room temperature, the black powder was collected for subsequent characterization and catalytic testing.

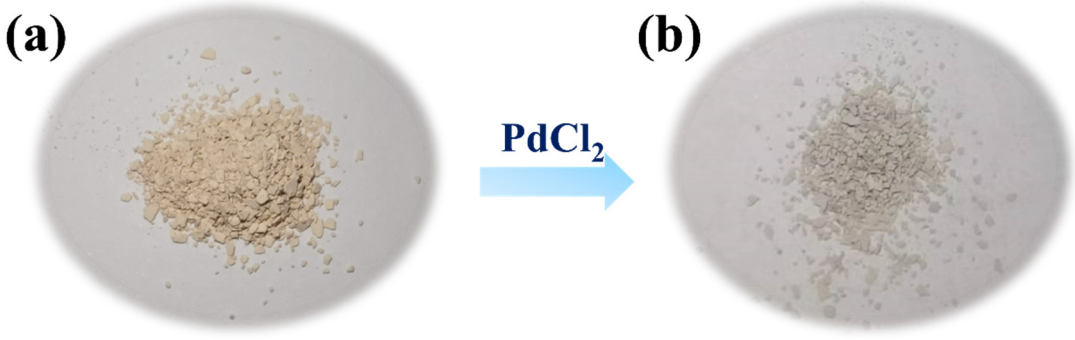

Figure S1. The color of UiO-66–NH_2 (a) and $PdCl_2$/UiO-66–NH_2 (b).

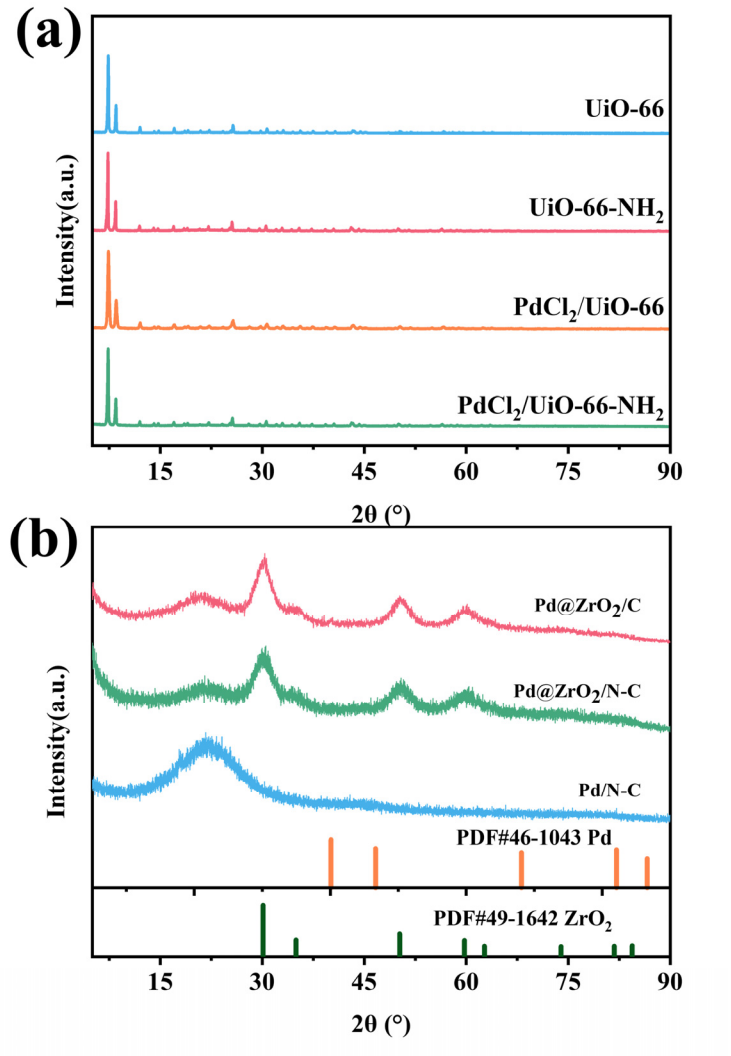

Figure S2. XRD patterns of (a) UiO-66, UiO-66–NH_2, $PdCl_2$/UiO–66 and $PdCl_2$/UiO-66–NH_2, and (b) Pd@ZrO_2/C, Pd@ZrO_2/N–C and Pd/N–C, respectively.

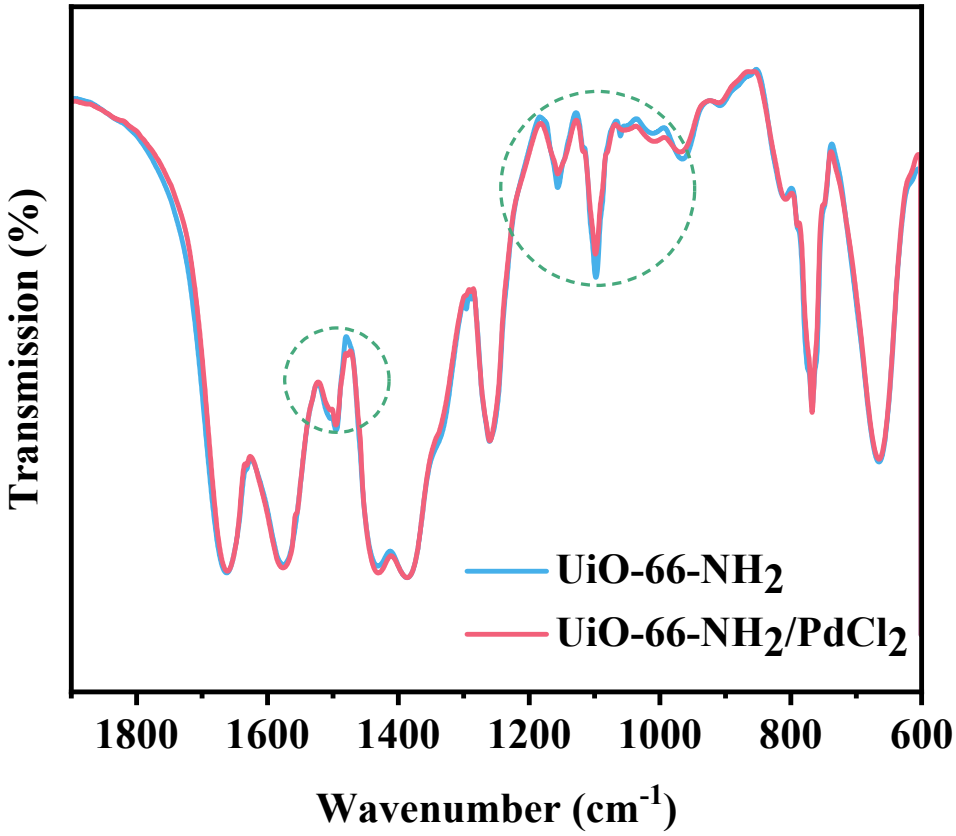

Figure S3. FT-IR spectra of UiO-66–NH_2 and $PdCl_2$/UiO-66–NH_2, respectively.

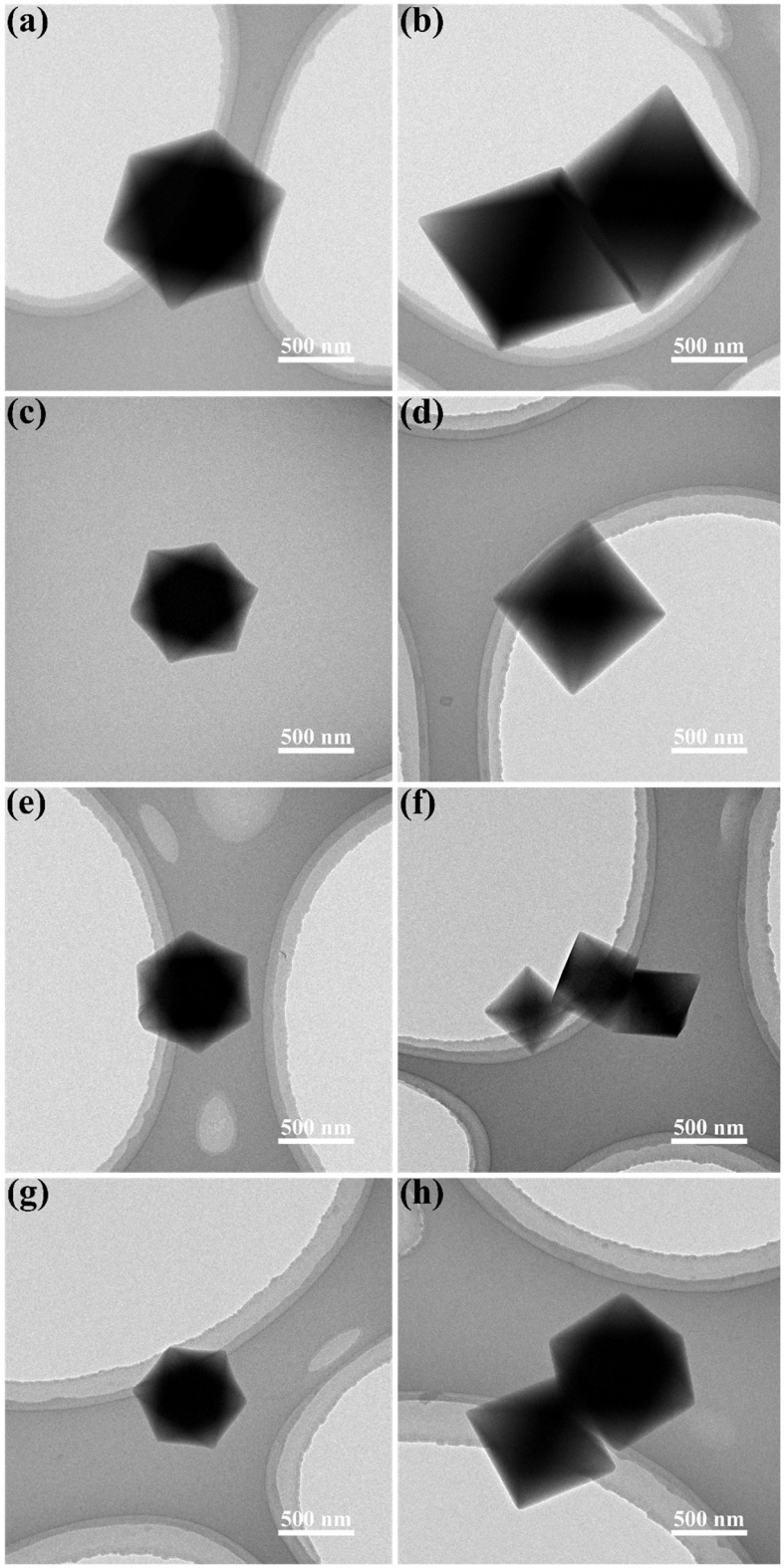

Figure S4. TEM images of (a) and (b) UiO-66, (c) and (d) UiO-66–NH_2, (e) and (f) $PdCl_2$/UiO-66 and (g) and (h) $PdCl_2$/UiO-66–NH_2.

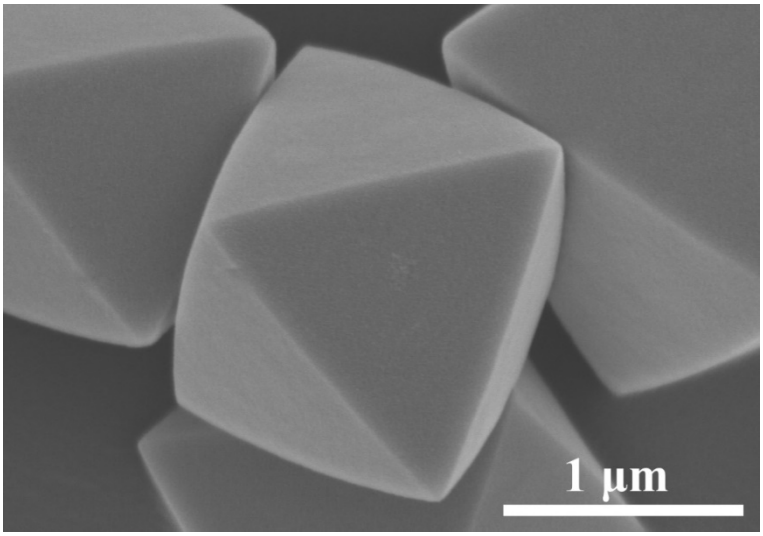

Figure S5. SEM image of Pd@ZrO_2/N–C.

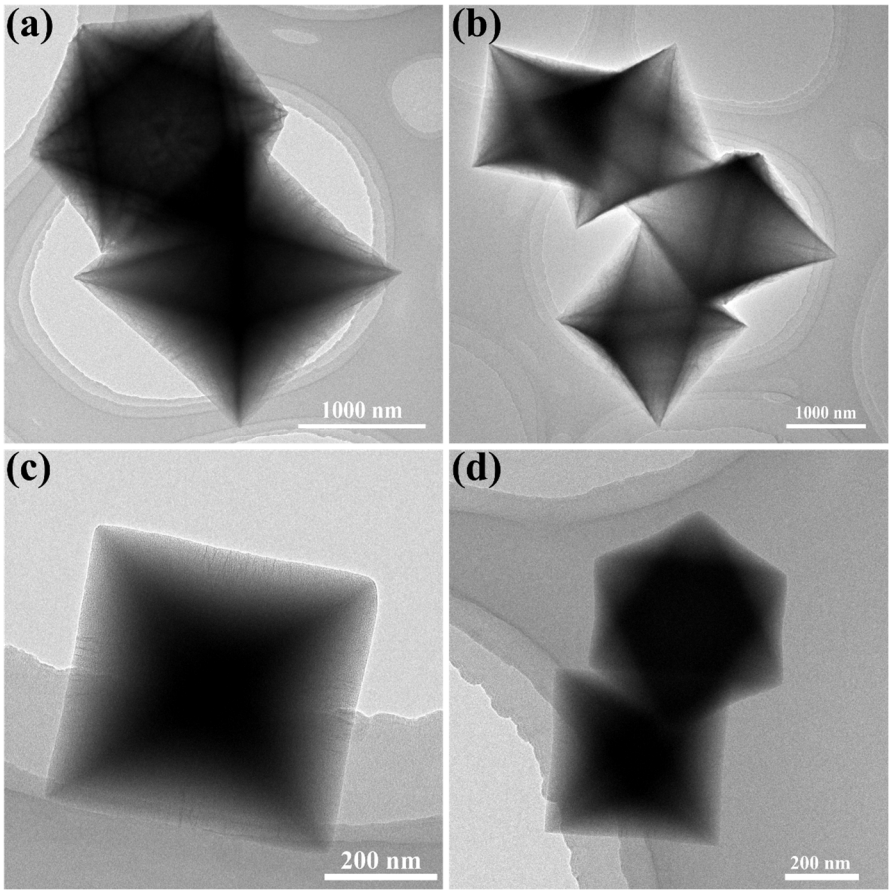

Figure S6. TEM images of (a) and (b) Pd@ZrO_2/C, (c) and (d) ZrO_2/N–C.

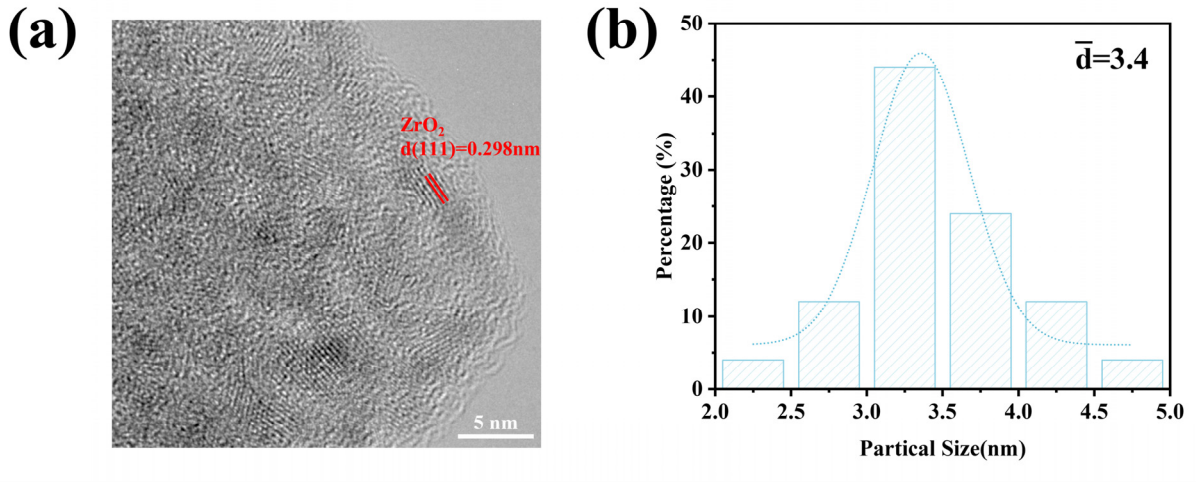

Figure S7. a) HRTEM image and (b) the statistic diagram of ZrO_2 particle sizes of Pd@ZrO_2/N–C sample.

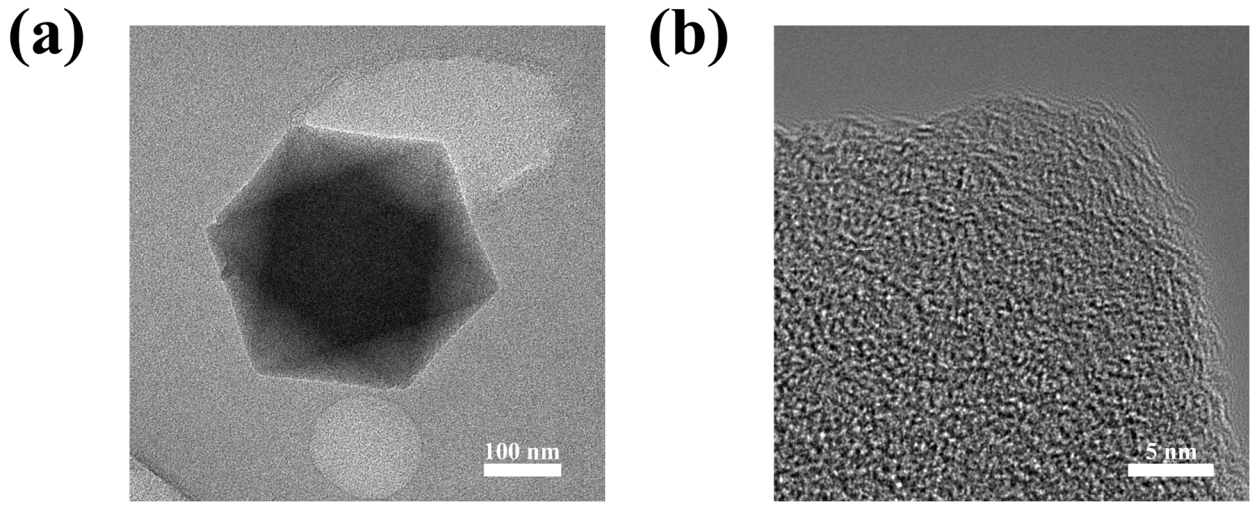

Figure S8. a) TEM image and (b) HRTEM image of Pd/N–C.

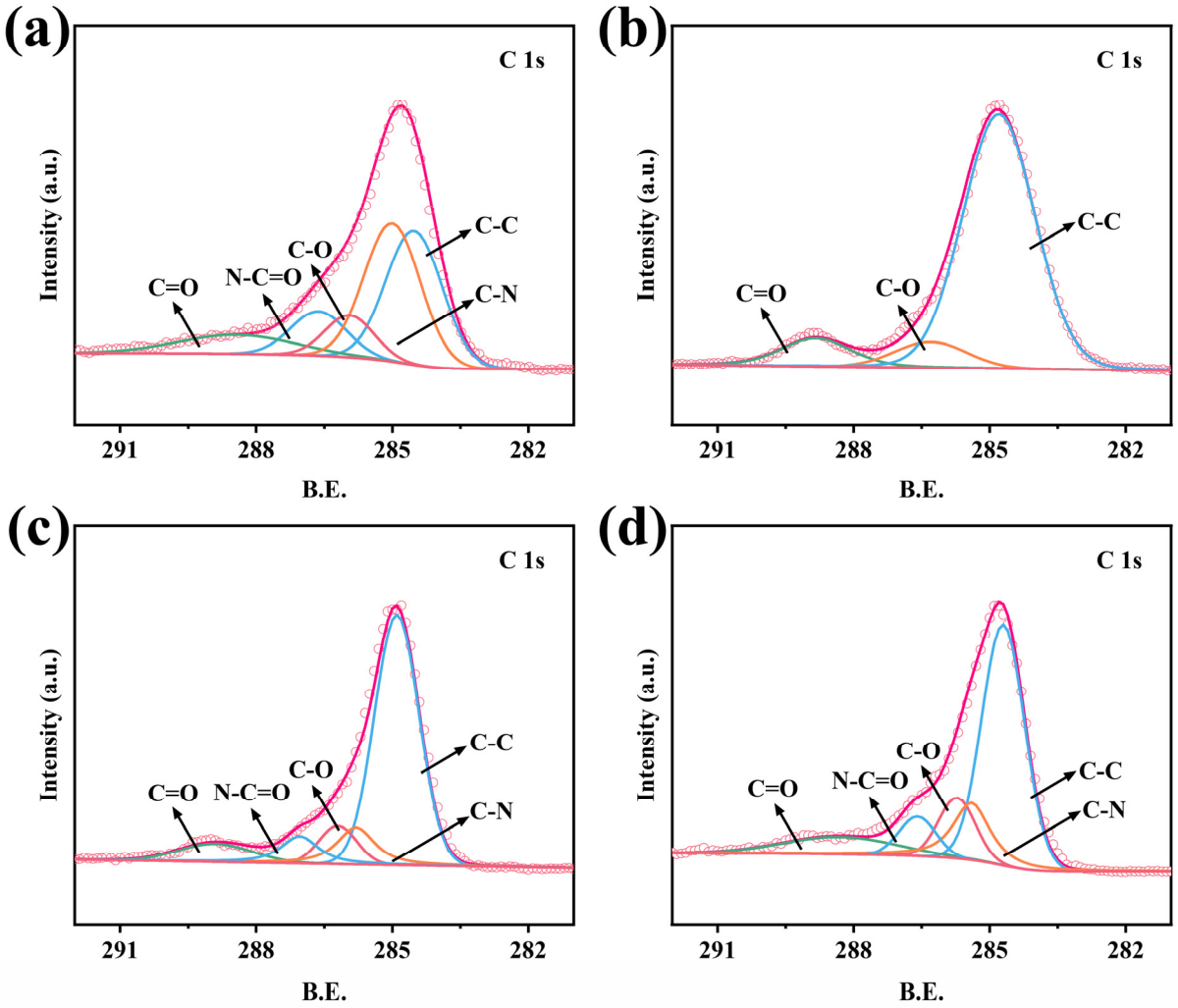

Figure S9. C 1s XPS spectra of (a) ZrO_2/N–C (b) Pd@ZrO_2/C, (c) Pd@ZrO_2/N–C and (d) Pd/N–C, respectively.

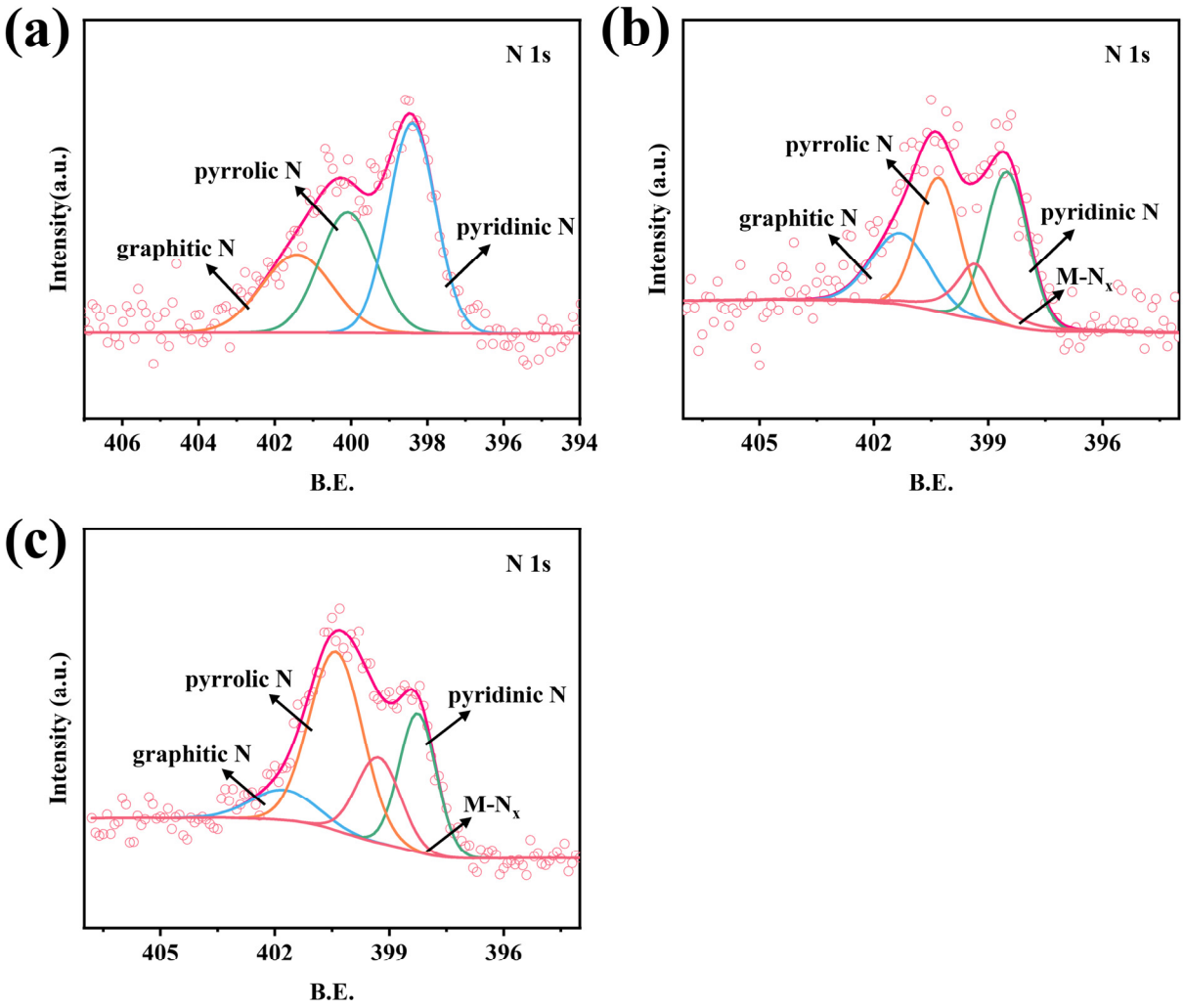

Figure S10. N 1s XPS spectra of (a) ZrO_2/N–C, (b) Pd@ZrO_2/N–C and (c) Pd/N–C, respectively.

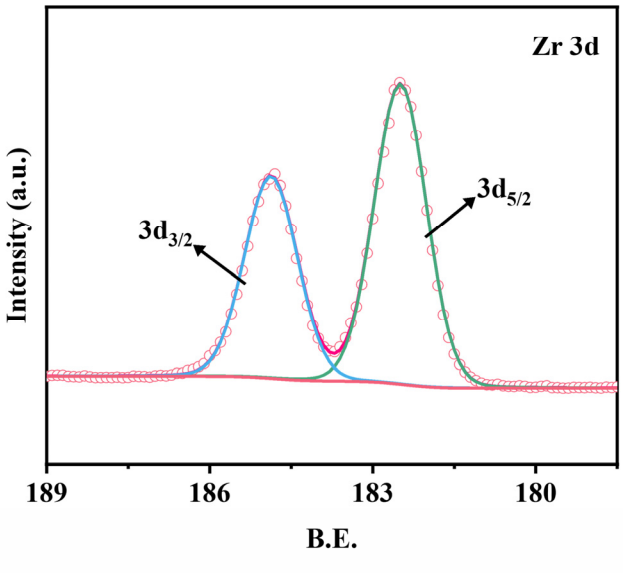

Figure S11. Zr 3d XPS spectrum of Pd@ZrO_2/N–C.

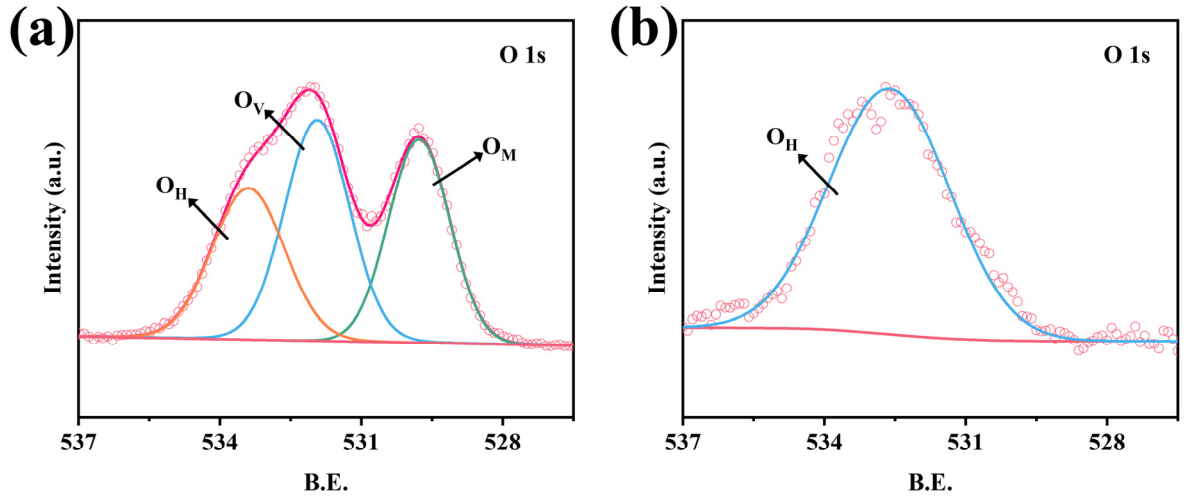

Figure S12. O 1s XPS spectra of (a) Pd@ZrO_2/C and (b) Pd /N–C, respectively.

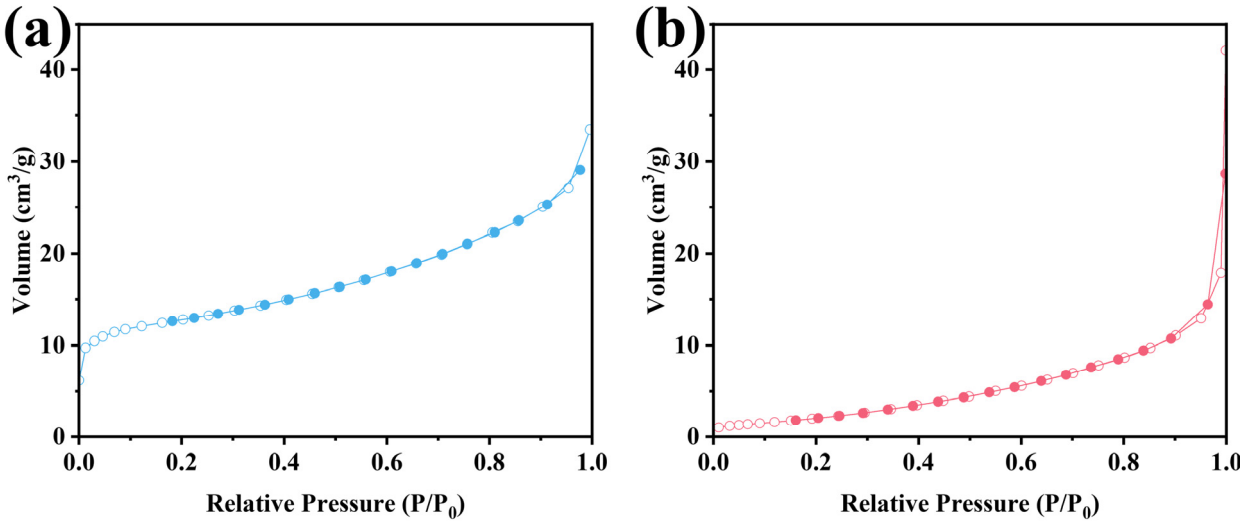

Figure S13. N_2 adsorption/desorption isotherms of (a) Pd@ZrO_2/N–C and (b) ZrO_2/N–C.

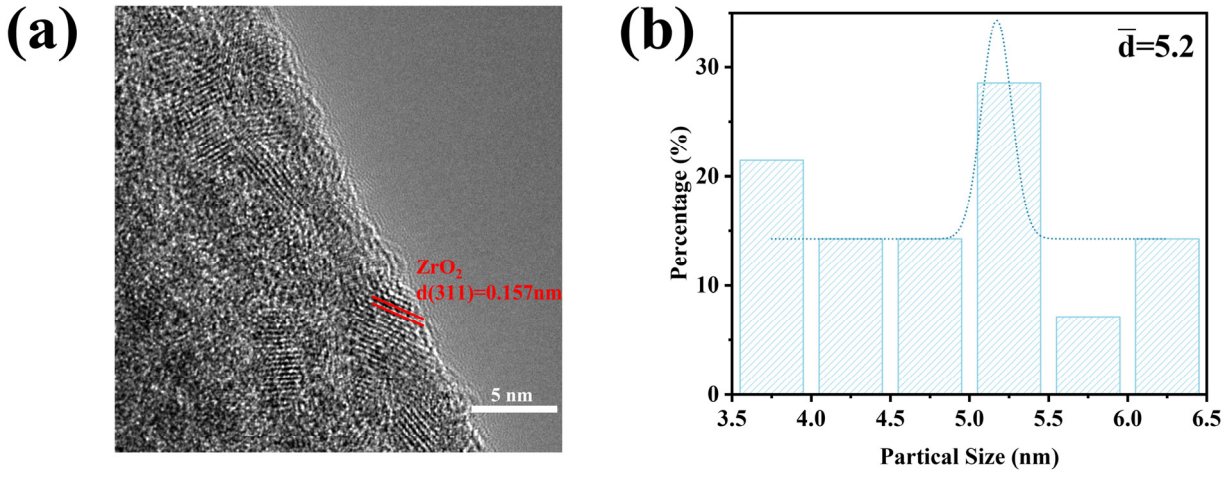

Figure S14. a) HRTEM image and (b) the statistic diagram of ZrO_2 particle sizes of ZrO_2/N–C sample.

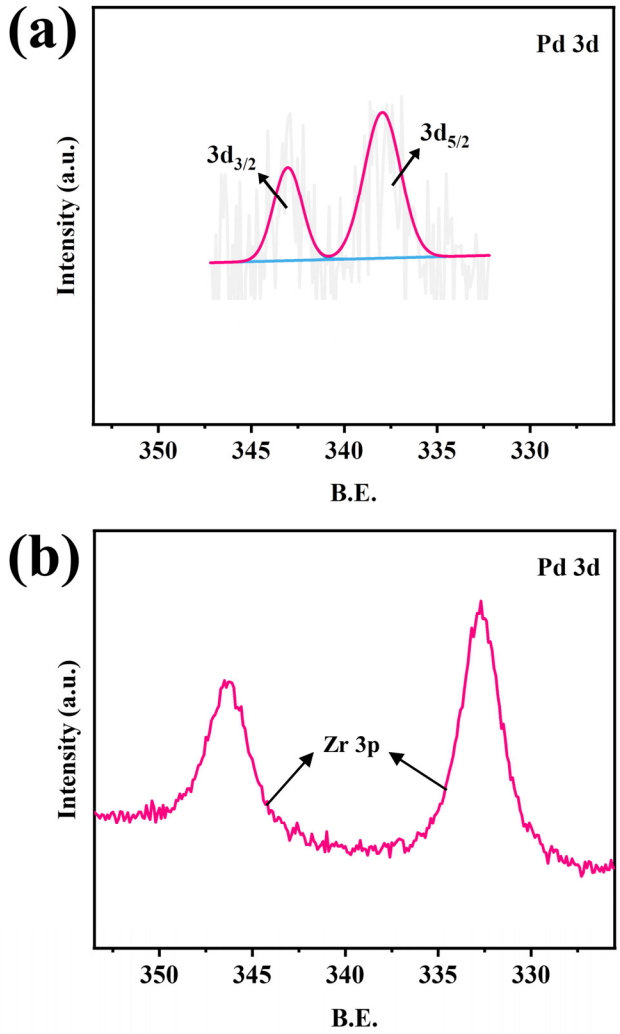

Figure S15. Pd 3d XPS spectra of (a) Pd/N–C and (b) Pd@ZrO2/C, respectively.

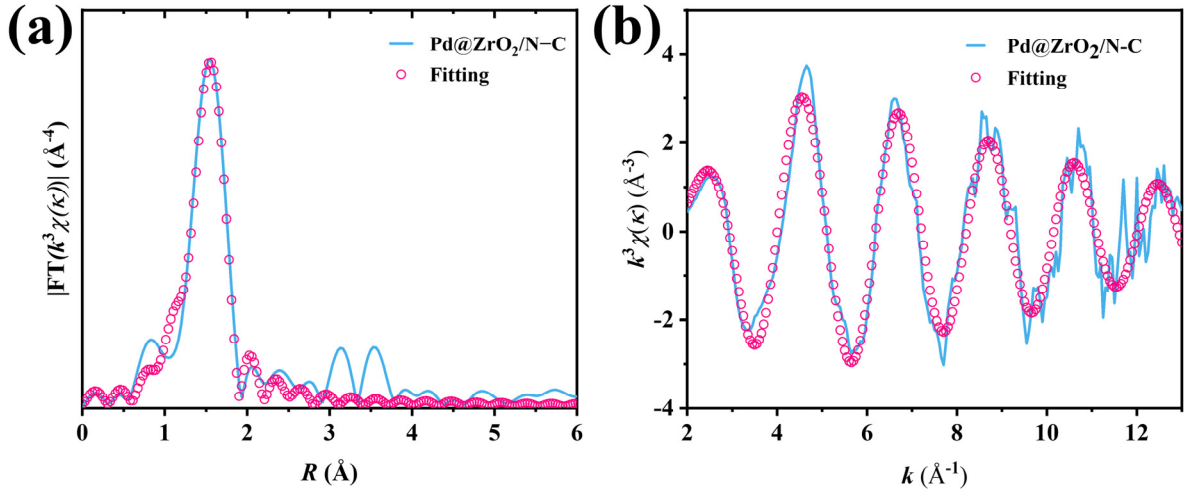

Figure S16. a) EXAFS R space fitting curve (circles) and the experimental data (blue line) of Pd@ZrO2/N–C. (b) EXAFS k space fitting curve (circles) and the experimental data (blue line) of Pd@ZrO2/N–C.

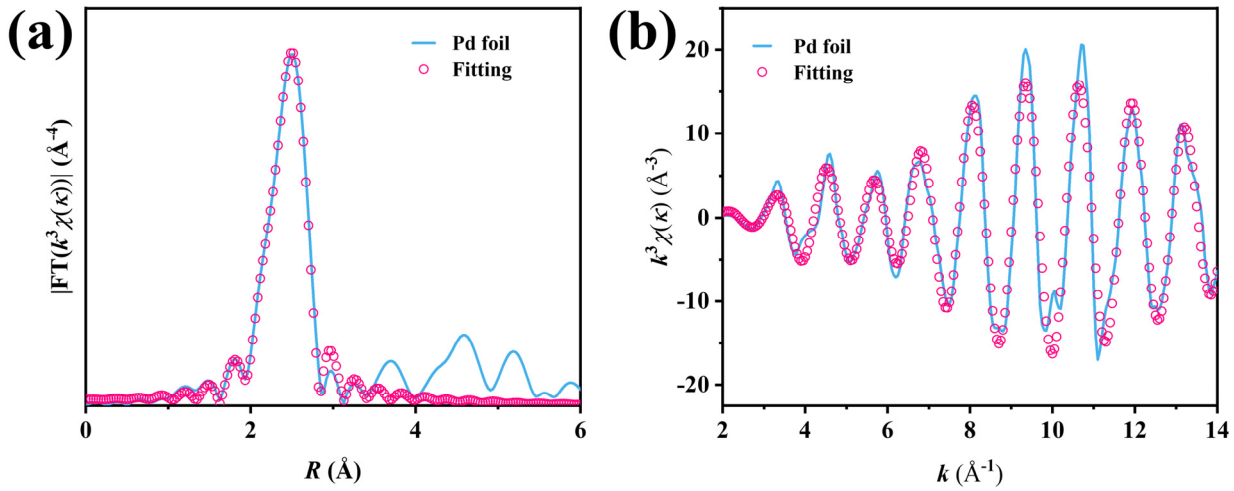

Figure S17. a) EXAFS R space fitting curve (circles) and the experimental data (blue line) of Pd foil. (b) EXAFS k space fitting curve (circles) and the experimental data (blue line) of Pd foil

Table S1 EXAFS fitting parameters at the Pd K-edge for various samples (S_0^2=0.818).

Sample	Shell	N[a]	R(Å)[b]	$\sigma^2\times10^3$(Å^2)[c]	ΔE_0 (eV)[d]	R factor
Pd foil	Pd-Pd	12*	2.740±0.001	5.5±0.2	3.9±0.3	0.0041
sample	Pd-O/N	3.3±0.5	2.003±0.011	4.1±1.3	4.1±2.2	0.0166

[a]N: coordination numbers; [b]R: bond distance; [c]σ^2: Debye-Waller factors; [d] ΔE_0: the inner potential correction. R factor: goodness of fit.

Table S2. Comparison of the turnover frequencies reported over palladium catalysts in the Suzuki coupling.

Entry	Catalyst	Reaction conditions	Yield (%)	TOF(h^{-1})	Ref.
1	Pd@ZrO_2/N–C	iodobenzene/ phenylboronic acid/ H_2O : EtOH/ K_2CO_3/80 °C /4h/0.03 mol% Pd	99	825	This work
2	Pd-N_3C_1-SAC	iodobenzene/ phenylboronic acid/ DME/K_2CO_3/110 °C/24 h/1 mol% Pd	99	4	[1]
3	MOP-BPY (Pd)	4-bromoanisole /phenylboronic acid /MeOH:H_2O/Na_2CO_3 (441 μmol)/80 °C/12 h/0.01 mol% Pd	95	822	[2]
4	Pd-SAs/3DOM-CeO_2	iodobenzene/ phenylboronic acid/ EtOH:H_2O/K_2CO_3/25 °C/4 h/0.1 mol% Pd	92	751	[3]
5	Pd-ECN	bromobenzene/phenyl boronic acid pinacol ester/ DME: H_2O /K_2CO_3/ 120 °C /10 min/ 5 wt% Pd	57	549	[4]

References

1. Liu, J.; Chen, Z.; Liu, C.; Zhang, B.; Du, Y.; Liu, C.-F.; Ma, L.; Xi, S.; Li, R.; Zhao, X.; Song, J.; Sui, X. Z.; Yu, W.; Miao, L.; Jiang, J.; Koh, M. J.; Loh, K. P. Molecular engineered palladium single atom catalysts with an M-C_1N_3 subunit for Suzuki coupling. *J. Mater. Chem. A* **2021**, *9*, 11427-11432.
2. Kim, S.; Jee, S.; Choi, K. M.; Shin, D.-S. Single-atom Pd catalyst anchored on Zr-based metal-organic polyhedra for Suzuki-Miyaura cross coupling reactions in aqueous media. *Nano Res.* **2020**, *14*, 486-492.
3. Tao, X.; Long, R.; Wu, D.; Hu, Y.; Qiu, G.; Qi, Z.; Li, B.; Jiang, R.; Xiong, Y. Anchoring positively charged Pd single atoms in ordered porous ceria to boost catalytic activity and stability in Suzuki coupling reactions. *Small* **2020**, *16*, 2001782.
4. Chen, Z.; Vorobyeva, E.; Mitchell, S.; Fako, E.; Ortuno, M. A.; Lopez, N.; Collins, S. M.; Midgley, P. A.; Richard, S.; Vile, G.; Perez-Ramirez, J. A heterogeneous single-atom palladium catalyst surpassing homogeneous systems for Suzuki coupling. *Nat. Nanotechnol.* **2018**, *13*, 702-707.